

Article

Monitoring of Carriageway Cross Section Profiles on Forest Roads: Assessment of an Ultrasound Data Based Road Scanner with TLS Data Reference

Michael Starke ^{1,*} , Anton Kunneke ² and Martin Ziesak ¹

¹ Division Forest Sciences, School for Agricultural, Forest and Food Sciences HAFL, Bern University of Applied Sciences, Länggasse 85, CH-3052 Zollikofen, Switzerland; martin.ziesak@bfh.ch

² Department of Forest and Wood Science, Stellenbosch University, Stellenbosch 7599, South Africa; ak3@sun.ac.za

* Correspondence: Michael.Starke@bfh.ch

Abstract: Forest roads are an important element in forest management as they provide infrastructure for different forest stakeholder groups. Over time, a variety of road assessment concepts for better planning were initiated. The monitoring of the surface cross-section profile of forest roads particularly offers the possibility to take early action in restoring a road segment and avoiding higher future costs. One vehicle-based monitoring system that relies on ultrasound sensors addresses this topic. With advantages in its dirt influence tolerance and high temporal resolution, but shortcomings in horizontal and vertical measuring accuracy, the system was tested against high resolution terrestrial laser scanner (TLS) data to find and assess working scenarios that fit the low-resolution measuring principle. In a related field test, we found low correct road geometry interpretation rates of 54.3% but rising to 91.2% under distinctive geometric properties. The further applied line- and segment-based method used to transform the TLS data to fit the road scanner measuring method allows the transfer of the road scanner evaluation principle to point-cloud or raster data of different origins.

Keywords: ultrasound sensors; road scanner; terrestrial laser scanning; TLS; forest road maintenance; forest road monitoring; crowned road surface



Citation: Starke, M.; Kunneke, A.; Ziesak, M. Monitoring of Carriageway Cross Section Profiles on Forest Roads: Assessment of an Ultrasound Data Based Road Scanner with TLS Data Reference. *Forests* **2021**, *12*, 1191. <https://doi.org/10.3390/f12091191>

Academic Editors: Robert Keefe, Andrea R. Proto, Mihai Nita and Stelian Alexandru Borz

Received: 23 July 2021

Accepted: 26 August 2021

Published: 2 September 2021

Publisher's Note: MDPI stays neutral with regard to jurisdictional claims in published maps and institutional affiliations.



Copyright: © 2021 by the authors. Licensee MDPI, Basel, Switzerland. This article is an open access article distributed under the terms and conditions of the Creative Commons Attribution (CC BY) license (<https://creativecommons.org/licenses/by/4.0/>).

1. Introduction

Information about forest road condition has become increasingly important. Not only basic road accessibility, but also an intensified use of forest roads by other forest stakeholder groups [1] can thereby influence the need for maintenance intensity and frequency [2]. Questions, from basic usability and stability, up to the assessment of high-quality road construction standards needed for, e.g., recreational aspects [3,4], can therefore be driving factors for collecting additional information about a road condition status to be able to take action within given financial constraints [2].

The therefore selected parameters describing the road condition vary with the quality standards and maintenance concepts. Thus, destruction-free monitoring concepts can include the road surface roughness in its different definitions and recording methods [3,5,6], direct wear expressions of the road surface [7–9], or the road geometry in comparison with a targeted road design. The road geometry, however, is an especially important part of road quality assessment. Its design determines the drainage of the road surface and is crucial for avoiding longitudinal water accumulation which can result in accelerated erosion effects [4,10–12]. Thus, it helps to identify potential construction problems even before severe damage in the form of wear expressions on a forest road surface appears.

One data source that is used to describe forest road geometries is originated from airborne laser scanning. Caused by the given spatial resolution, the area of application is found on larger-scale road geometries [13] or focuses on strong geometrical expressions

such as the ditch as drainage system [7]. Higher potential and more possibilities in monitoring the road geometries can be achieved by changing the recording distance, and therefore the resolution of the data [14]. Specially equipped vehicles for road condition monitoring which are mostly based on LiDAR systems already exist, but are mostly designed for sealed road surfaces [15], creating data with low temporal resolution, as a separate, cost-intensive measuring vehicle is required for data collection. To utilise the advantage of the close-range recording with higher temporal resolution, alternative measuring principles have emerged in the forest sector with the aim to close the gap between temporal and spatial resolution to serve alternative monitoring concepts.

In this context, a different vehicle-based and low-cost road scanning concept, which is applied as an ultrasound sensor-based setup, was developed [16,17]. The aim of this system is to be used in the day-to-day business when mounted on the back of a forester's car to collect frequent information about the road condition status by describing the road surface geometry in combination with its surface roughness. In comparison with other near-range sensor setups suitable for forest use, most of which are based on LiDAR or photogrammetric systems [3,9], this system alternatively operates with ultrasound distance sensors to detect the cross-section profile of a forest road's carriageway surface, and so addresses annual maintenance concepts to detect and further restore a functional lateral water drainage of the carriageway [18]. The lens-less ultrasound measurement principle allows the user to continue measurements under muddy or dusty measuring conditions, but again limits the resolution of the measurement. This drawback was already noted in earlier tests conducted under laboratory conditions [19].

The present study focuses on the recording of the carriageway cross-section profiles on forest roads, particularly of a single-laned design. In a field testing, vehicle-based data from the ultrasound sensor setup of the road scanner are compared with high resolution data collected with a terrestrial laser scanning (TLS) system, to find areas of application to substitute high resolution data with low-cost and -quality data of high temporal resolution. For the data comparison, the recording method of the road scanner was adopted to TLS data to describe cross-sections within defined road segments in order to assess lateral water flow over parallel lane sections. The specific objectives of the study were:

- (a) to adopt the lane-based measuring principle of the ultrasound sensor-based road scanner to high resolution LiDAR data, to assess the quality of the lower resolution data of the road scanner, and to transfer the lane-based recording method to other data sources; and
- (b) to use data filtering to identify data application scenarios for using the road scanner setup for forest road surface monitoring purposes.

2. Materials and Methods

For the study, a gravel road surface was recorded with two measurement principles: the ultrasound-sensor-based, low resolution road scanner, installed at the back of a car and measuring in movement, and the terrestrial laser scanner in a static measuring setup. To accommodate the different data resolutions, the road was split into equally sized segments in longitudinal direction to obtain comparable road segments for further evaluation. The road characteristic per segment was then described through the height differences between sensor position related lanes on the road surface that are used to describe an inclined or crowned road surface profile. Subsequently, the algebraic sign of the lateral road inclination was compared between the measurement principles to describe the direction of potential water flow. The percentage of equal classification of both principles was then evaluated to find a comparable road description setup.

The study was carried out in Switzerland on a gravel road (46°59'27.6" N 7°27'50.4" E), separating two agricultural fields in an open area on flat terrain ($\Delta z_{\max} = 3.35$ m for the whole road), to focus on the surface recording principle and to rule out forest canopy influences. The road had a total length of 440 m and a width of 2.2 m (outer edges of the visible lanes). It was straight, but with one 90-degree-exceeding corner at two thirds of the

length (segments no. 29, 30). The cross-section profile did not follow a distinct crowned profile, but was characterized by existing or emerging vegetation in the middle of the road, combined with a beginning of rut expression. In the area of two local vertical drainage installations (segments no. 19, 29), road surface erosion expressions started appearing. There was no subsequent water drainage for lateral nor longitudinal direction.

The road was first measured with a TLS system followed by the low-resolution ultrasound sensors (US). With 5 US (MaxBotics Inc., Fort Mill, Brainerd, MN, USA: MaxSonar MB7040) that are built into the road scanner [19,20], the vertical distance between the scanner bar and the road surface was measured and the cross-section profile of the road recorded. The sensor distance was equally set up with a 0.45 m spacing (Figure 1) and the scanner was mounted in a height of 0.4 m on the car hitch for vertical measuring towards the road surface. Four of the sensors used were the MB7040 XLI2C-MaxSonar-WR type. At position 4, a MB7040 XLI2C-MaxSonar-WRC sensor equipped with a ceramic cone head was mounted and expected to provide a more focused measuring cone of the road surface. The sensors were triggered in a round-robin measurement principle and a 10 Hz trigger frequency of each sensor to minimize reflection interference between the sensors. All sensors provided a resolution of 1 cm in vertical direction [20] where the distance value is calculated by the sensor internally in a pre-processing step. Erratic values above 0.65 m were excluded in advance of the data evaluation step, as these values relate to technical errors and cannot be explained by specific, distance-related situations. With a u-blox NEO-M8N GNSS sensor, the spatial reference was added simultaneously to the measurements in a 1 Hz resolution, with location interpolation for in-between recordings. For higher accuracy, an external active magnetic antenna was used, which was mounted on the car roof. This setup reaches an accuracy of at least 1.5 m in driving direction, which was verified by a shock-inducing control point for the built-in acceleration sensor, that was placed on the test track. The road was then recorded in 14 overall passes (repetitions) at a strived constant driving speed of 20 km h⁻¹. In total, 13 passes contained valid GPS values for the further spatial evaluation.

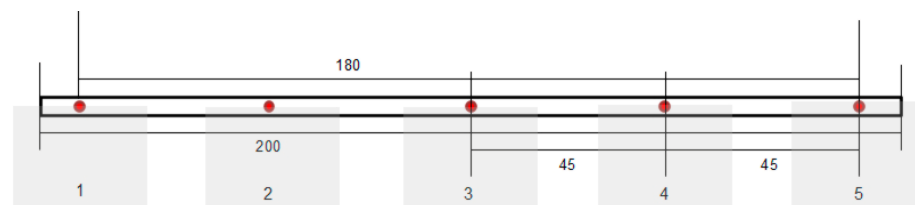


Figure 1. Ultrasonic sensor setup and dimensions of the mounted road scanner bar (cm), including the spacing of the ultrasound sensors (red), with a central mounting point at sensor 3, in combination with their maximal detection beam width (grey).

For reference measurements, the road was scanned with a TLS system FARO 3D X330 in a chained scanning setup of 21 scans, positioned on the carriageway in a scanning height of 1.5 m and a varying scanning distance of around 25 m. For the point-cloud registration and to improve the basic internal GPS referencing, the position of 13 scanning targets were additionally calculated from theodolite measurements, referenced to an official geographic survey point, located near the road entrance.

After the separate scans were combined to a single point cloud, road scanner related sensor lanes were constructed following the known sensor spacings built up after one manually defined sensor lane. After the lanes were located, subsets of the point cloud were extracted as 0.05 m wide strips (Figure 2).

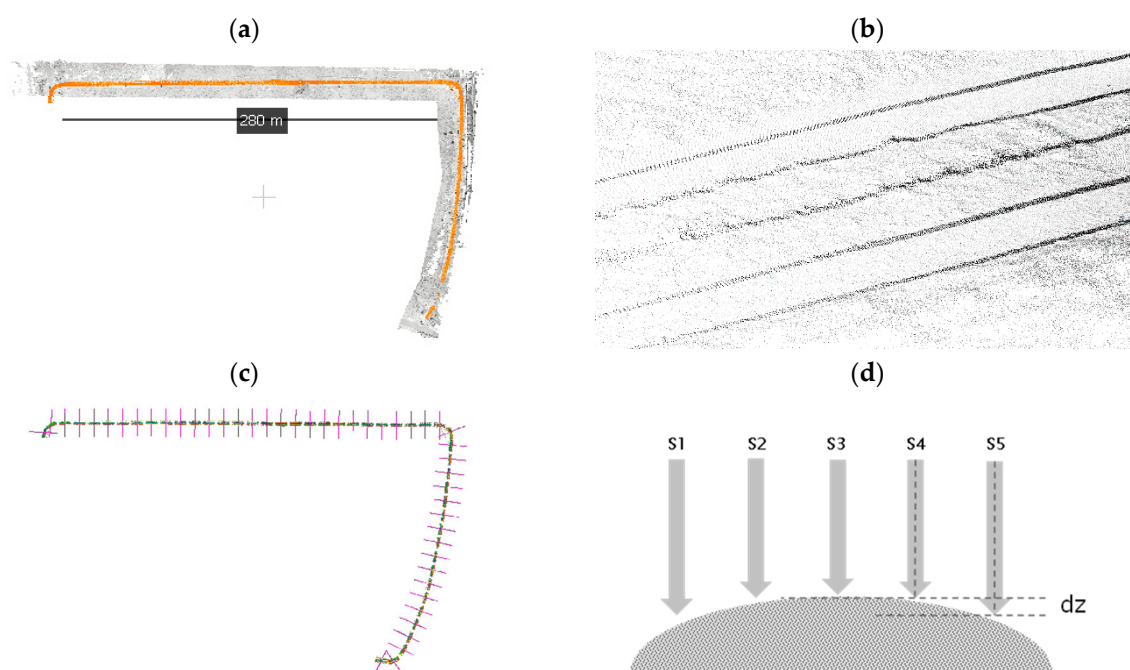


Figure 2. Data processing and evaluation steps: (a) combination of terrestrial laser scanning (TLS, grey background area) and road scanner measurements (orange); (b) reference sensor lane extraction (black) from the TLS data background (grey); (c) longitudinal segmentation of both data sources with 2 m spacing; and (d) calculating the mean height difference (dz) to represent the lateral water-flow between two sensor lanes, visualized between sensor 4 (S4) and sensor 5 (S5) of one segment.

Next, the recordings of both measurement types were similarly segmented into 44 sections of 8 m with a spacing of 2 m between the segments. The spacing was used to minimize GPS inaccuracies that may influence adjacent sections and could not be excluded with the open field setup. The minimum segment length of 8 m is limited by the number of sample points that are collected by the road scanner and are expected to be counted within one road segment. Despite the multiple repetition of the measurements of the road scanner, the created input data are differently characterised by number of data points, referenced to all 44 road segments (Table 1).

Table 1. Overview of the collected data, including the number of valid data points per sensor lane within the defined segments.

	TLS Measurements	Road Scanner Measurements
Recording date	4 July 2019	5 July 2019
Number of scans	21 single scans	13 repetitions
Number of segments	44	44
Number of data points	769'537 (for extr. sensor lanes)	25'814
Sum of valid data points	Sensor 1 → 174'711	Sensor 1 → 5'473
	Sensor 2 → 145'448	Sensor 2 → 4'996
	Sensor 3 → 137'993	Sensor 3 → 5'039
	Sensor 4 → 140'674	Sensor 4 → 5'324
	Sensor 5 → 170'711	Sensor 5 → 4'982

As the lateral geometrical expression of the road is the focus of the study, the relative height differences in z direction (dz) between the mean sensor values of two sensors each were compared (Figure 2). For each segment separately, the result could then be interpreted as direction for a potential lateral waterflow between the related two sensor

lanes with an information gap reflecting uncertainty in between the sensor lanes and the data averaging for the segment length. For the evaluation, the algebraic sign of the dz value from the different data sources was used. This characterises the inclination direction with the minimum required resolution for water flow interpretation. When comparing the different data sources, a “positive match” was noted in case of a match of the sign of the relative heights. This means, for the US sensor data, respectively the TLS sensor lanes n , $k = 1,2,3,4,5$:

$$(S_{\text{TLS}}(n) - S_{\text{TLS}}(k)) \cdot (S_{\text{US}}(n) - S_{\text{US}}(k)) > 0 \Rightarrow \text{pos. match (1), with } n < k, \quad (1)$$

$$(S_{\text{TLS}}(n) - S_{\text{TLS}}(k)) \cdot (S_{\text{US}}(n) - S_{\text{US}}(k)) < 0 \Rightarrow \text{no match (0), with } n < k, \quad (2)$$

with $S(n)$ as relative mean z value per segment of the road surface of the first, and $S(k)$ the mean elevation of the second sensor (lane) considered.

As a last evaluation step, and to overcome low mean detection percentage, the introduction of an evaluation threshold as data filter was further tested. For this, all sensor combinations and segments were grouped for a combined dataset to separate thresholds that influence the height difference recognition.

All statistical analyses were carried out with the statistic software R (R Development Core Team 2020). To check the repetition accuracy of the recordings, the Dunnett’s Test was used for multi-group comparison. Further, the effects of different scenarios that influence the matching rate of the data were tested with the Wilcoxon Rank Sum Test, which suited the testing preconditions.

3. Results

3.1. Data Quality and Mean Detection Rate

On average, 9.75 values (SD = 13.2, min = 1, max = 273, 1.22 points m^{-1}) per segment, repetition, and sensor were recorded with the road scanner. This point density equals 24.4 points m^{-2} , upscaled from the sensor lane area and ignoring spaces between the sensor lanes. For the TLS data, 3497.9 (SD = 3997.6, min = 45, max = 18549) values per segment and sensor lane (8745 points m^{-2}) were taken. The difference between the mean values of the segments were characterized with a SD = 2.17 cm for the road scanner and SD = 3.06 cm for the TLS data.

The repetition accuracy of the road scanner shows constant results. For all sensors, the repetition measurements do not differ significantly ($p < 0.05$) regarding the mean values per segment (Dunnett’s Test, with first recording as control data). In a confidence interval with $\alpha = 0.1$, sensor 4 with the ceramic cone shows significant differences in the repetition in two cases. It has the lowest SD = 1.89 cm of vertical values compared to the other sensors (total sensor SD = 2.06 cm).

The average recorded height differences between the sensors and recording types for the entire road are shown in Figure 3 and Table 2. The crown profile (S1_3 and S3_5) is expressed with, on average, 3.54 cm between these sensor lanes, which equals a lateral inclination of 3.93% of the carriageway from the highest point in the middle to the lowest point on the outer lane. The related ultrasound sensors recognized a lateral height difference of 1.23 cm on average, with its highest peak on sensor 2 showing a different picture (Figure 3). The TLS-derived mean profile shows higher inter-quantile ranges for all sensors compared to the US-derived road profile.

For all possible sensor combinations, a matching of the sensor pairs of the different data origins averaged 54.3% (SD = 22.3) for the mean segment values. A possible connection between the detection percentage and the mean dz value is visible for the higher correlated sensors referring to a maximum expected dz value (S1_3, S3_5, Table 2, Figure 4). These sensor combinations reach a detection percentage of 72.1%.

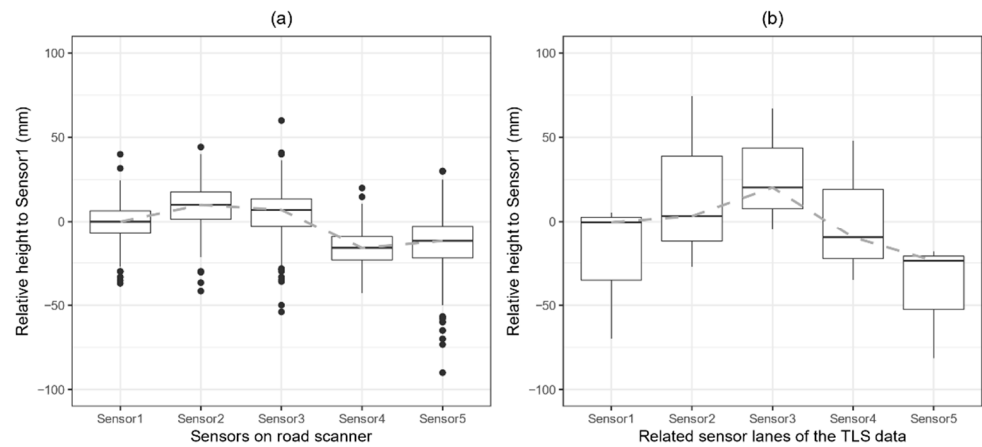


Figure 3. Visualization of the mean road cross-section profiles for the whole road of the different recording types: (a) low-resolution, ultrasound measurement and (b) TLS measurement.

Table 2. Mean sensor (S) height differences ($S_{n-k} = S_n - S_k$) of the recording type road scanner (US), and terrestrial laser scanner (TLS), and the compartment on positive matches of sensor pairs considering a positive or negative height difference.

Sensor Combination	S1_2	S1_3	S1_4	S1_5	S2_3	S2_4	S2_5	S3_4	S3_5	S4_5
US data (cm)	-0.998	-0.637	1.510	1.191	0.361	2.508	2.189	2.146	1.828	-0.319
TLS data (cm)	-1.545	-3.497	-2.003	0.081	-1.952	-0.459	1.626	1.493	3.578	2.084
Correlation between US and TLS datasets	0.24	0.17	0.02	-0.06	0.01	-0.01	0.08	0.21	0.21	0.06
Positive detections (%)	67.3	71.3	31.2	43.6	38.2	44.7	55.1	72.3	73.0	46.3

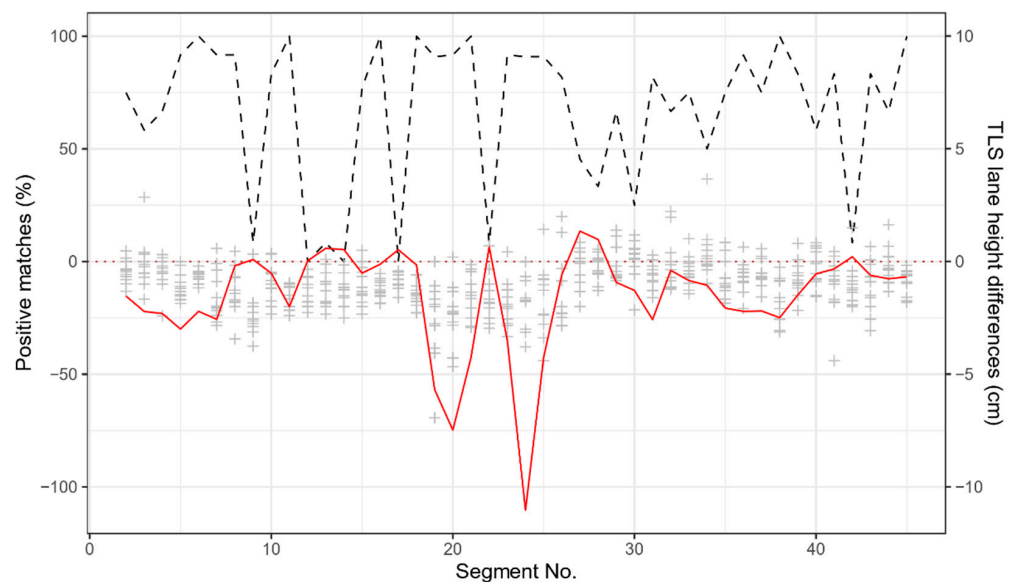


Figure 4. Positive inclination matches of sensor height differences between road scanner and TLS data, per repetition and segment (dashed line), including the absolute height difference (cm) derived from the TLS data (red) and from the road scanner data (grey crosses) for sensor combination S1_2 (mean $dz_{TLS} = -1.54$ cm, $dz_{US} = -1.00$ cm with 67.3% detection rate).

When plotting the dz value and the detection percentage of only one sensor pair, the correlation behaviour between the TLS and the US data becomes visible (Figure 4). When a certain dz value is exceeded, the detection rate tends to sharply increase (segments 17–24, Figure 4). A moderate positive correlation between the absolute, mean TLS–dz values per sensor pair and the matching percentage (0.48) supports this connection.

3.2. Threshold Value Filtering Effects

For a minimum evaluated mean difference of +1 cm, the detection rate rises significantly from 54.3% to 78.8% ($p = 0.005$, Wilcox Test) (Figure 5a). When applying an absolute value as a filter to consider negative and positive deviations, or setting the filter on the US data, no further sudden increments of the rate of detection matches are observed. The difference of setting filters on positive or absolute values on the lower resolution road scanner data has a minor effect compared on the TLS data, and is still characterized by a high standard deviation of values.

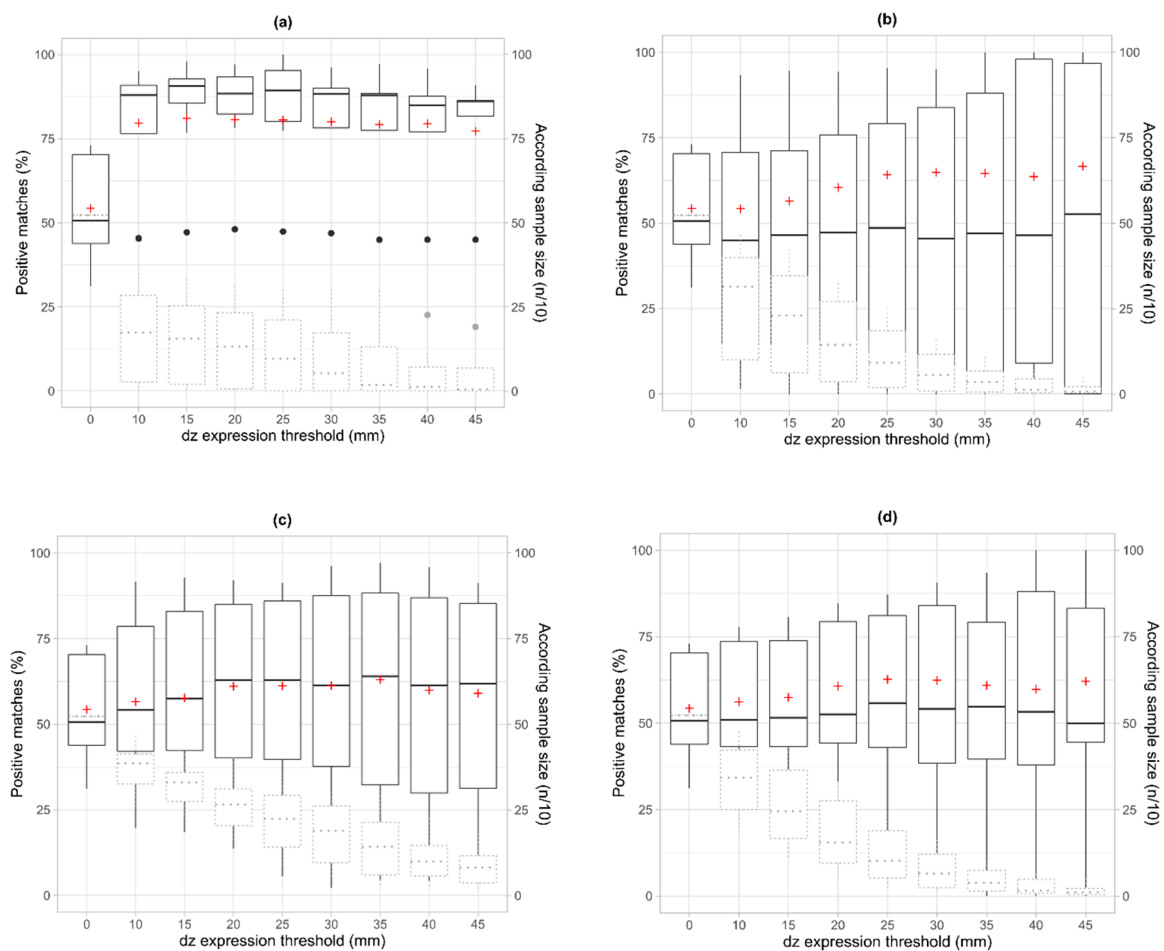


Figure 5. Development of positive matches (solid line boxes, cross marks the mean of all observations) and remaining sample segments (dash-lined boxes) between the ultrasound sensor data and the TLS data, when setting filters on a dz value for (a) only positive dz values of the TLS data, (b) only positive dz values on the ultrasound data, (c) absolute values of the TLS data, and (d) absolute values of the ultrasound data.

As for application purposes only internal data filter are usable; a maximum detection percentage with 62.5% can be reached by applying a 2.5 cm threshold for evaluation.

3.3. Sensor Lane Filtering Effect

As some sensor combinations are expected to show no height differences due to the road profile expression, these combinations can be excluded before applying the system

when the basic road geometry is known. In a single-laned, crowned road profile, these combinations are the same height levelled sensor-pair 1 and 5 and, respectively, sensor-pair 2 and 4. The best results can thus be reached with 71.6% in combination with a 3 cm height difference filter (Figure 6).

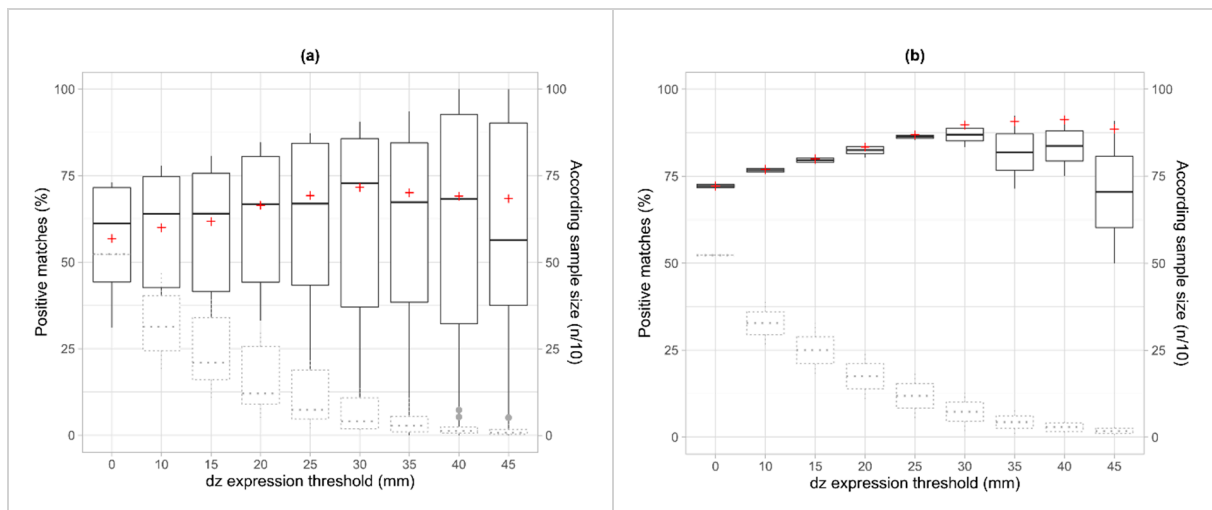


Figure 6. Development of positive matches (solid line box) and remaining sample size between the ultrasound sensor data and the TLS data, when setting filters on a dz value and (a) excluding horizontally aligned sensor pairs (S1_5 and S2_4) or (b) only considering max dz value sensor pairs (S1_3 and S3_5).

When differently applied, the maximum expected height difference of a crowned road profile is observed with the system over the highest and the lowest sensor point locations (S1_3 and S3_5), the detection rate rises from 54.3% without filter to 72.2%, and reaches a maximum of 91.2% with an additional 4 cm dz filter applied. For higher filter rates, the remaining sample size ($n = 35$) cannot be considered as high enough to keep up the trend. Evaluating a filter up to 4 cm, the according regression model shows a 5.2% higher matching rate per 1 cm dz filtering (adj. R-squared = 0.97, $p < 0.000$).

4. Discussion

With the segment- and lane-based method applied, we presented a way to simplify LiDAR data and make it comparable with different data sources as the road scanner measurements. The concept of directly describing the lateral inclination thereby substitutes the method of data comparison over quality parameters as used in further studies [21] due to the earlier integration of false positive and false negative values considered as incorrect interpretation.

Longitudinal geometry parameters that could override lateral geometry expressions in the evaluation process are minimized in advance, as the road inclination in driving direction is considered equal for all lanes. A balanced distribution of datapoints in longitudinal direction is thereby important for a successful data preparation. With the point density of 24.4 points per square meter, upscaled from an assumed 5 cm sample-stripe that represents the minimal detection width of the sensor, the road scanner data point density was relatively high in comparison with airborne laser scanning (ALS) data with up to 16 points per m^2 [22]. This sample drawing method could therefore also be a possible enhancement of ALS-based evaluation concepts in steeper terrain [8].

Between the different data sources, the mean road profiles showed basic similarities in their geometric expression, but with lower average values in z direction at the middle sensor position of the ultrasound sensor data. As this sensor lane was partly influenced by emerging vegetation, the relation between the ultrasound measuring principle and the vegetation could have caused that effect. This observation is supported by the results of earlier tests under laboratory conditions, where the detection of vegetation with the

ultrasound sensors was also not possible [19]. This difference in the measuring principles between ultrasound and LiDAR can lead to an advantage of this sensor selection, as the direct road surface can potentially be separated with the ultrasound measurements.

The limited vertical resolution of the US sensors, caused by the sensor-internal distance calculation, made the comparison of the measurement principles challenging. When a filter from -1 to $+1$ cm as factory resolution of the sensor was set separately on each dataset, only small improvements of the matching data percentage were observed. Only with the filter set exclusively on positive height difference expressions did a significant rise of the matching percentage appear. This can be caused by multiple influence factors, such as a missing homogenous distribution of the sample data within the segments, in combination with a longitudinal road inclination, a broken sensor, or a missing horizontal alignment of the scanner bar. As no one-sided expressed road inclination was noted, and the sensor data showed no inconsistencies, the alignment of the scanner bar seems to cause the trend of the measured data.

To discuss a suitable application of the system with the identified measuring peculiarities, the consideration of typical forest influences and deviating road construction parameters seem necessary. As the study was conducted in open terrain, the aimed advantage of high accuracies achieved within the spatial referencing exceeded accuracies reachable under forest canopy conditions [23]. As the lane-based information of the road scanner is relative information dependent on the sensor spacing, this issue only affects the allocation accuracy in driving direction, or the basic spatial join of the data with the road assessed. Accuracy limitations are, thus, not crucial for an implementation of the system, as segment lengths can be adjusted independently of statistical evaluation intervals. Furthermore, to transfer the road scanner results to forest conditions, common lateral road inclinations of forest roads must also be known, as road construction variants that can influence the earlier noted data quality are common, related to the expressed dz values observed. Former studies mention that, in road construction, a carriageway inclination in lateral direction should be expressed with a slope of 5–8% for crowned road surfaces [24,25]. For the given sensor spacing, this would imply an expected dz value of 2.25 cm for neighbored sensor pairs, or 4.5 cm when only every second sensor is considered. In the present study, the mean dz value of the road was below 1.77 cm. The reference road that was selected for this study can thus be rated as ambitious, regarding its overall profile characteristics and the given measuring behaviour of the system. When applying the system in these situations, higher detection rates related to the raw data can therefore be assumed.

As a further measure to raise data reliability, filters can alternatively be set on dz values for specific sensor combinations to focus on the road's maximum dz expressions. When the road is designed as a single driving lane, and the vehicle used for the measurement can pass the road in the middle of the crowned surface profile, the highest dz values are given between the middle sensor and the outer sensors. Applied in this manner, the previously mentioned skipping of one sensor lane raised the detection percentages of the true geometry up to over 91%, and with this showed good results for application. On the downside, geometric information in between the longer sensor distances is thereby lost, which needs to be considered in the overall monitoring purpose.

A fundamental absence of a crowned profile, however, makes the application of the system challenging. As the detection rates rise with dz filters used, the targeted geometry or road damage of the observation must at least exceed the thresholds of the filters applied. Additionally, the valuably recognized sensor-skipping approach to raise the dz value can no longer be used, which forces the system to be used with US data filtering only.

5. Conclusions

The method of a striped and segment-based analysis for assessing different cross-section monitoring principles was demonstrated to also be possible on a LiDAR-based road recording concept. This method can be especially helpful for comparing measurement

principles with one dataset missing exact horizontal spatial reference, or for overcoming longitudinal inclination influences on existing methods.

The road scanner presented itself as diverse working system. With its characteristic to screen vegetation on the road surface, advantages in comparison with the reference TLS measurements occurred that need further attention. Satisfying data quality for application was found for a geometry expression threshold of 3.5 cm. This is in accordance with literature-based suggestions of a lateral road inclination for single laned crowned road profiles in the existing sensor setup, which makes the system best fitted for these situations to record a forest road carriageway geometry with high temporal resolution.

Author Contributions: Conceptualization, M.S., A.K. and M.Z.; methodology, M.S.; data collection, M.S. and A.K.; validation, M.S.; formal analysis, M.S.; resources, M.Z.; data curation, M.S.; writing—original draft preparation, M.S.; writing—review and editing, M.S., A.K. and M.Z.; visualization, M.S.; and project administration, M.Z. All authors have read and agreed to the published version of the manuscript.

Funding: The APC was funded by the Bern University of Applied Sciences Open Science Office.

Data Availability Statement: The data presented in this study are available on request from the corresponding author.

Conflicts of Interest: The authors declare no conflict of interest.

References

1. Toscani, P.; Sekot, W.; Holzleitner, F. Forest Roads from the Perspective of Managerial Accounting—Empirical Evidence from Austria. *Forests* **2020**, *11*, 378. [[CrossRef](#)]
2. Dodson, E.M. Challenges in Forest Road Maintenance in North America. *Croat. J. For. Eng.* **2021**, *42*, 107–116. [[CrossRef](#)]
3. Marinello, F.; Proto, A.R.; Zimbalatti, G.; Pezzuolo, A.; Cavalli, R.; Grigolato, S. Determination of forest road surface roughness by Kinect depth imaging. *Ann. For. Res.* **2017**, *60*, 217–226. [[CrossRef](#)]
4. Dobias, J. Forest road erosion. *J. For. Sci.* **2012**, *51*, 37–46. [[CrossRef](#)]
5. Brown, M.; Mercier, S.; Provencher, Y. Road Maintenance with Opti-Grade[®]: Maintaining Road Networks to Achieve the Best Value. *Transp. Res. Rec. J. Transp. Res. Board* **2003**, *1819*, 282–286. [[CrossRef](#)]
6. Svenson, G.A.; Fjeld, D. The impact of road geometry and surface roughness on fuel consumption of logging trucks. *Scand. J. For. Res.* **2015**, *31*, 526–536. [[CrossRef](#)]
7. Kiss, K.; Malinen, J.; Tokola, T. Forest road quality control using ALS data. *Can. J. For. Res.* **2015**, *45*, 1636–1642. [[CrossRef](#)]
8. Kiss, K.; Malinen, J.; Tokola, T. Comparison of high and low density airborne lidar data for forest road quality assessment. *ISPRS Ann. Photogramm. Remote Sens. Spat. Inf. Sci.* **2016**, *III-8*, 167–172. [[CrossRef](#)]
9. Zhang, C. Monitoring the Condition of Unpaved Roads with Remote Sensing and Other Technology: Final Report for US DOT DTPH56-06-BAA-0002, Brookings. 2008. Available online: https://rosap.ntl.bts.gov/view/dot/36464/dot_36464_DS1.pdf (accessed on 22 January 2021).
10. Heinimann, H.R. Aggregate-surfaced Forest Roads—Analysis of Vulnerability Due To Surface Erosion. In Proceedings of the IUFRO/FAO Seminar on Forest Operations in Himalayan Forests with Special Consideration of Ergonomic and Socio-Economic Problems, Thimphu, Bhutan, 20–23 October 1997; pp. 30–37. Available online: <http://www.uni-kassel.de/upress/online/frei/978-3-933146-12-0.volltext.frei.pdf#page=39> (accessed on 1 September 2021).
11. Napper, C. Soil and Water Road-Condition Index—Field Guide. 2008. Available online: <https://www.fs.fed.us/t-d/ ///pubs/pdf/08771806.pdf> (accessed on 21 January 2021).
12. Moll, J.; Copstead, R.; Johansen, D.K. Traveled Way SurfaceShape. 1997. Available online: https://www.fs.fed.us/eng/pubs/html/wr_p/97771808/97771808.htm (accessed on 21 January 2021).
13. White, R.A.; Dietterick, B.C.; Mastin, T.; Strohman, R. Forest Roads Mapped Using LiDAR in Steep Forested Terrain. *Remote Sens.* **2010**, *2*, 1120–1141. [[CrossRef](#)]
14. Talbot, B.; Pierzchała, M.; Astrup, R. Applications of Remote and Proximal Sensing for Improved Precision in Forest Operations. *Croat. J. For. Eng.* **2017**, *38*, 327–336. Available online: <http://www.crojfe.com/site/assets/files/4090/talbot.pdf> (accessed on 21 July 2021).
15. Ahlin, K.; Granlund, J.; Lindstrom, F. Comparing road profiles with vehicle perceived roughness. *Int. J. Veh. Des.* **2004**, *36*, 270–286. [[CrossRef](#)]
16. Rommel, D.; Ziesak, M. Automatisierte Zustandserfassung von Güterwegen—Bedienbarkeitsaspekte des Instrumentariums [Automated condition assessment of freight roads—Usability aspects of the instrumentation]. In Proceedings of the Informatik in der Land-, Forst- und Ernährungswirtschaft: Fokus: Komplexität versus Bedienbarkeit, Mensch-Maschine-Schnittstellen; Referate der 35. GIL-Jahrestagung, Geisenheim, Germany, 23–24 February 2014; Ruckelshausen, A., Ed.; Gesellschaft für Informatik: Bonn, Germany, 2015; pp. 153–156, ISBN 978-3-88579-632-9. (In German)

17. Ziesak, M. System zur Ermittlung des Zustandes von Insbesondere Unbefestigten Fahrtrassen, Wie z. B. Forststraßen Oder Güterwegen [System for Determining the Condition of, in Particular, Unpaved Roadways, Such as Forest Roads or Freight Roads], 10 July 2014. Available online: <https://register.dpma.de/DPMAREgister/pat/register?AKZ=1020142134242> (accessed on 21 July 2021). (In German)
18. Begus, J.; Pertlik, E. Guide for Planning, Construction and Maintenance of Forest Roads. 2017. Available online: <http://www.fao.org/3/i7051e/i7051e.pdf> (accessed on 21 July 2021).
19. Starke, M.; Ziesak, M.; Rommel, D.; Hug, P. An automated detection system for (forest) road conditions. In Proceedings of the FORMEC 2016—From Theory to Practice: Challenges for Forest Engineering, Warsaw, Poland, 4–7 September 2016; pp. 261–266. Available online: <https://www.formec.org/images/formec2016/proceedings-formec-poland-2016.pdf> (accessed on 21 July 2021).
20. MaxBotix. Datasheet for the I2CXL-MaxSonar-WR Sensor Line. Available online: https://www.maxbotix.com/documents/I2CXL-MaxSonar-WR_Datasheet.pdf (accessed on 10 February 2015).
21. Azizi, Z.; Najafi, A.; Sadeghian, S. Forest Road Detection Using LiDAR Data. *J. For. Res.* **2014**, *25*, 975–980. [[CrossRef](#)]
22. Hruža, P.; Mikita, T.; Janata, P. Monitoring of Forest Hauling Roads Wearing Course Damage Using Unmanned Aerial Systems. *Acta Univ. Agric. Silvic. Mendel. Brun.* **2016**, *64*, 1537–1546. [[CrossRef](#)]
23. Naasset, E.; Jonmeister, T. Assessing Point Accuracy of DGPS Under Forest Canopy Before Data Acquisition, in the Field and After Postprocessing. *Scand. J. For. Res.* **2002**, *17*, 351–358. [[CrossRef](#)]
24. Kuonen, V. *Wald- und Güterstrassen: Planung—Projektierung—Bau: Planung—Projektierung—Bau. [Forest and Freight Roads: Planning—Projecting—Construction]*; ETH Zurich: Pfaffhausen, Switzerland, 1983. [[CrossRef](#)]
25. Hölldorfer, B. Einfach, aber wirkungsvoll-das R2005-Gerät [Simple but effective-the R2005 device]. *LWF Aktuell* **2007**, *59*, 30–31. Available online: https://www.lwf.bayern.de/mam/cms04/service/dateien/a59_einfach_aber_wirkungsvoll_das_r2_geraet.pdf (accessed on 21 July 2021). (In German)